Journal of Sound and Vibration (2002) **252**(3), 429–442
doi:10.1006/jsvi.2001.3693, available online at http://www.idealibrary.com on IDEAL®

FREE VIBRATIONS OF SIMPLY SUPPORTED AND MULTILAYERED MAGNETO-ELECTRO-ELASTIC PLATES

E. PAN

Structures Technology, Inc., 543 Keisler Drive, Suite 204, Cary, NC 27511, U.S.A.
E-mail: Ernian_Pan@yahoo.com

AND

P. R. HEYLIGER

Department of Civil Engineering, Colorado State University, Fort Collins, CO, U.S.A.

(*Received* 1 *September* 2000, *and in final form* 19 *March* 2001)

Analytical solutions are derived for free vibrations of three-dimensional, linear anisotropic, magneto-electro-elastic, and multilayered rectangular plates under simply supported edge conditions. For any homogeneous layer, we construct the general solution in terms of a simple formalism that resembles the Stroh formalism, from which any physical quantities can be solved for given boundary conditions. In particular, the dispersion equation that characterizes the relationship between the natural frequency and wavenumber can be obtained in a simple form. For multilayered plates, we derive the dispersion relation in terms of the propagator matrices. The present solution includes all previous solutions, such as piezoelectric, piezomagnetic, and purely elastic solutions as special cases, and can serve as benchmarks to various thick plate theories and numerical methods used for the modelling of layered composite structures. Typical natural frequencies and mode shapes are presented for sandwich piezoelectric/piezomagnetic plates. It is shown clearly that some of the modes are purely elastic while others are fully coupled with piezoelectric/piezomagnetic quantities, with the latter depending strongly upon the material property and stacking sequence. These frequency and mode shape features could be of particular interest to the analysis and design of various "smart" sensors/actuators constructed from magneto-electro-elastic composite laminates.

1. INTRODUCTION

Due to their analytical nature, exact solutions of vibrations of simply supported (layered) plates are of particular value. These solutions can predict exactly the natural frequencies of the system and the corresponding mode shapes, particularly, as the physical quantities are near or across the interface of dissimilar material layers, and can thus be used to check the accuracy of various numerical methods for more complicated problems [1]. For anisotropic elastic composites, Srinivas *et al.* [2], and Srinivas and Rao [3] derived the classic vibration solutions for both cylindrical and rectangular plates. While Pan [4] introduced the propagator matrix method [5] to handle the corresponding multilayered cases, Noor and Burton [6] solved the laminated plate problems with general anisotropy.

Recent development of piezoelectric ceramics has stimulated considerable studies on the electric and mechanical behaviors of piezoelectric structures. Again, analytical solutions, though under certain assumptions, are still desirable. Ray and co-workers [7, 8] and

Heyliger and co-workers [9, 10] extended the free vibration solution of simply supported elastic plates to the corresponding piezoelectric case.

More recent advances are the smart or intelligent materials where piezoelectric and/or piezomagnetic materials are involved. These materials have the ability of converting energy from one form to the other (among magnetic, electric, and mechanical energies). Furthermore, composites made of piezoelectric/piezomagnetic materials exhibit a magnetoelectric effect that is not present in single-phase piezoelectric or piezomagnetic materials [11–13].

Very recently, Pan [14] presented an exact closed-form solution for the static deformation of the layered piezoelectric/piezomagnetic plate. In that approach, the homogeneous solution was derived based on a new and simple formalism resembling the Stroh formalism, and the propagator matrix method was used to handle the multilayered case. Some numerical examples in that paper clearly indicate that piezoelectric/piezomagnetic material possesses some special features that may be useful in the smart structure analysis and design.

In this paper, we extend the analytical method of Pan [14] to the free vibration of three-dimensional, linear anisotropic, magneto-electro-elastic, simply supported, and multilayered rectangular plates. First, we derive the general solution in a homogeneous plate in terms of the Stroh-type formalism. In order to treat multilayered plates, the propagator matrix method is again introduced with which the corresponding multilayered solution has an elegant and simple expression. To the best of the authors' knowledge, this is the first time that the free vibrations of a piezoelectric and magnetostrictive plate under simply supported conditions are analytically studied. The present solution includes all previous solutions, such as the piezoelectric, piezomagnetic, and purely elastic solutions as special cases. Since the present solution is exact, it can serve as the benchmark for various thick plate theories and approximate numerical methods, such as the finite and boundary element methods.

Our formulation has been checked for the free vibration of a purely elastic and a piezoelectric homogeneous plate. For the purely elastic case, our formulation predicts exactly the same natural frequencies as those by the previous model. As for the piezoelectric case, we are again able to predict the exact natural frequencies. Furthermore, we have noted that three of the six natural frequencies, two symmetric and one antisymmetric, are the same for different electric boundary conditions on the top and bottom surfaces. Consequently, we are able to identify these three modes as those corresponding to the purely elastic plate.

We finally applied our solution to the sandwich plate made of piezoelectric $BaTiO_3$ and magnetostrictive $CoFe_2O_4$. For the four cases of the sandwich piezoelectric/magnetostrictive plates considered in this paper (i.e., B only, F only, B/F/B, and F/B/F, with B standing for $BaTiO_3$ and F for $CoFe_2O_4$), we observed that for the same mode, the natural frequencies for the four cases are quite different. Also, similar to the piezoelectric plate case, we found that some of the modes, either symmetric or antisymmetric, are purely elastic. That is, for these modes, piezoelectric/magnetostrictive coupling does not produce electric and magnetic potentials, and the elastic displacements are nearly identical in both the purely elastic and piezoelectric/magnetostrictive cases. We believe that these important features could be useful in the analysis and design of various "smart" sensors/actuators constructed from piezoelectric/magnetostrictive composites.

2. PROBLEM DESCRIPTION AND GOVERNING EQUATIONS

We consider an anisotropic, magneto-electro-elastic, and N-layered rectangular plate with horizontal dimensions L_x and L_y and total thickness H (in the vertical or thickness direction). We further assume that its four edges are simply supported (as can be observed from equations (6) and (8) given below). A Cartesian co-ordinate system $(x, y, z) \equiv (x_1, x_2, x_3)$ is attached to the plate in such a way that its origin is at one of the four corners on the bottom surface, with the plate being in the positive z region. Layer j is bonded by the lower interface z_j and the upper interface z_{j+1} with thickness $h_j = z_{j+1} - z_j$. It is obvious that $z_1 = 0$ and $z_{N+1} = H$. Along the interface, the extended displacement and traction vectors (to be defined later) are assumed to be continuous. One the top and bottom surfaces of the layered plate, zero traction and/or zero displacement are assumed.

We start with a linear, anisotropic, and magneto-electro-elastic solid for which the coupled constitutive relation can be written as [11–14]

$$\sigma_i = C_{ik}\gamma_k - e_{ki}E_k - q_{ki}H_k, \quad D_i = e_{ik}\gamma_k + \varepsilon_{ik}E_k + d_{ik}H_k, \quad B_i = q_{ik}\gamma_k + d_{ik}E_k + \mu_{ik}H_k, \tag{1}$$

where σ_i, D_i, and B_i are the stress, electric displacement, and magnetic induction (i.e., magnetic flux), respectively; γ_i, E_i, and H_i are the strain, electric field and magnetic field, respectively, C_{ij}, ε_{ij}, and μ_{ij} are the elastic, dielectric, and magnetic permeability coefficients, respectively, e_{ij}, q_{ij}, and d_{ij} are the piezoelectric, piezomagnetic, and magnetoelectric coefficients respectively. It is apparent that various uncoupled cases can be reduced from equation (1) by setting the appropriate coefficients to zero.

For an orthotropic solid to be considered in this paper, the material constant matrices of equation (1) are expressed by

$$[C] = \begin{bmatrix} C_{11} & C_{12} & C_{13} & 0 & 0 & 0 \\ & C_{22} & C_{23} & 0 & 0 & 0 \\ & & C_{33} & 0 & 0 & 0 \\ & & & C_{44} & 0 & 0 \\ & sym & & & C_{55} & 0 \\ & & & & & C_{66} \end{bmatrix}, \quad [e] = \begin{bmatrix} 0 & 0 & e_{31} \\ 0 & 0 & e_{32} \\ 0 & 0 & e_{33} \\ 0 & e_{24} & 0 \\ e_{15} & 0 & 0 \\ 0 & 0 & 0 \end{bmatrix}, \quad [q] = \begin{bmatrix} 0 & 0 & q_{31} \\ 0 & 0 & q_{32} \\ 0 & 0 & q_{33} \\ 0 & q_{24} & 0 \\ q_{15} & 0 & 0 \\ 0 & 0 & 0 \end{bmatrix}, \tag{2}$$

$$[\varepsilon] = \begin{bmatrix} \varepsilon_{11} & 0 & 0 \\ 0 & \varepsilon_{22} & 0 \\ 0 & 0 & \varepsilon_{33} \end{bmatrix}, \quad [d] = \begin{bmatrix} d_{11} & 0 & 0 \\ 0 & d_{22} & 0 \\ 0 & 0 & d_{33} \end{bmatrix}, \quad [\mu] = \begin{bmatrix} \mu_{11} & 0 & 0 \\ 0 & \mu_{22} & 0 \\ 0 & 0 & \mu_{33} \end{bmatrix}. \tag{3}$$

The general strain (using tensor symbol for the elastic strain γ_{ik})–displacement relation is

$$\gamma_{ij} = 0{\cdot}5(u_{i,j} + u_{j,i}), \quad E_i = -\phi_{,i}, \quad H_i = -\psi_{,i} \tag{4}$$

where u_i, ϕ, and ψ are the elastic displacement, electric potential, and magnetic potential respectively.

Assuming the absence of the body force, electric charge and current densities, the equations of motion can then be written as

$$\sigma_{ij,j} = \rho \frac{\partial^2 u_i}{\partial t^2}, \quad D_{j,j} = 0, \quad B_{j,j} = 0 \tag{5}$$

with ρ being the density of the material.

3. GENERAL SOLUTIONS

For a harmonic time-dependent motion $e^{i\omega t}$, we seek the solution of the *extended* displacement in the form of $\mathbf{u}(x, y, z;\ t) = \mathbf{u}(x, y, z)\,e^{i\omega t}$, where the time-independent displacement is expressed as

$$\mathbf{u} \equiv \begin{bmatrix} u_x \\ u_y \\ u_z \\ \phi \\ \psi \end{bmatrix} = e^{sz} \begin{bmatrix} a_1 \cos px \sin qy \\ a_2 \sin px \cos qy \\ a_3 \sin px \sin qy \\ a_4 \sin px \sin qy \\ a_5 \sin px \sin qy \end{bmatrix}. \tag{6}$$

and where s is the eigenvalue and a_i $(i = 1, \ldots, 5)$ the corresponding eigenvector to be determined, and

$$p = n\pi/L_x, \qquad q = m\pi/L_y \tag{7}$$

with n and m being two positive integers. In equation (6) and thereafter, the harmonic time-dependent factor $e^{i\omega t}$ has been omitted for simplicity.

Substitution of equation (6) into the strain–displacement relation (4) and subsequently into the constitutive relation (1) yields the *extended* traction vector

$$\mathbf{t} \equiv \begin{bmatrix} \sigma_{xz} \\ \sigma_{yz} \\ \sigma_{zz} \\ D_z \\ B_z \end{bmatrix} = e^{sz} \begin{bmatrix} b_1 \cos px \sin qy \\ b_2 \sin px \cos qy \\ b_3 \sin px \sin qy \\ b_4 \sin px \sin qy \\ b_5 \sin px \sin qy \end{bmatrix}. \tag{8}$$

Introducing two vectors

$$\mathbf{a} = [a_1, a_2, a_3, a_4, a_5]^t, \qquad \mathbf{b} = [b_1, b_2, b_3, b_4, b_5]^t, \tag{9}$$

we then find that vector $\mathbf{b}$ is related to $\mathbf{a}$ by the relation

$$\mathbf{b} = (-\mathbf{R}^t + s\mathbf{T})\,\mathbf{a} = -\frac{1}{s}(\mathbf{Q} + s\mathbf{R})\,\mathbf{a}, \tag{10}$$

where the superscript t denotes matrix transpose, and

$$\mathbf{R} = \begin{bmatrix} 0 & 0 & pC_{13} & pe_{31} & pq_{31} \\ 0 & 0 & qC_{23} & qe_{32} & pq_{32} \\ -pC_{55} & -qC_{44} & 0 & 0 & 0 \\ -pe_{15} & -qe_{24} & 0 & 0 & 0 \\ -pq_{15} & -qq_{24} & 0 & 0 & 0 \end{bmatrix}, \quad \mathbf{T} = \begin{bmatrix} C_{55} & 0 & 0 & 0 & 0 \\ & C_{44} & 0 & 0 & 0 \\ & & C_{33} & e_{33} & q_{33} \\ & Sym. & & -\varepsilon_{33} & -d_{33} \\ & & & & -\mu_{33} \end{bmatrix}, \tag{11}$$

$$\mathbf{Q} = \begin{bmatrix} -(C_{11}p^2+C_{66}q^2)+\rho\omega^2 & -pq(C_{12}+C_{66}) & 0 & 0 & 0 \\ & -(C_{66}p^2+C_{22}q^2)+\rho\omega^2 & 0 & 0 & 0 \\ & & -(C_{55}p^2+C_{44}q^2)+\rho\omega^2 & -(e_{15}p^2+e_{24}q^2) & -(q_{15}p^2+q_{24}q^2) \\ sym & & & \varepsilon_{11}p^2+e_{22}q^2 & d_{11}p^2+d_{22}q^2 \\ & & & & \mu_{11}p^2+\mu_{22}q^2 \end{bmatrix}. \tag{12}$$

The in-plane stresses and electric and magnetic displacements can be found using the strain–displacement relation (4), equations (6) and (8) [14].

Satisfaction of equation (5) yields the eigenproblem for the eigenvalue s and the corresponding eigenvector $\mathbf{a}$,

$$[\mathbf{Q} + s(\mathbf{R} + \mathbf{R}') + s^2\mathbf{T}]\,\mathbf{a} = 0, \tag{13}$$

where $\mathbf{R}' = -\mathbf{R}^t$.

It is noted that equation (13), derived for a simply supported plate, resembles the Stroh formalism [15, 16]. However, their solution structures are different because of the slightly different features of the involved matrices [14].

To solve eigenproblem (13), we can first recast it, with the aid of equation (10), into a 10×10 linear eigensystem

$$\mathbf{N}\begin{bmatrix} \mathbf{a} \\ \mathbf{b} \end{bmatrix} = s\begin{bmatrix} \mathbf{a} \\ \mathbf{b} \end{bmatrix}, \tag{14}$$

where

$$\mathbf{N} = \begin{bmatrix} -\mathbf{T}^{-1}\mathbf{R}' & \mathbf{T}^{-1} \\ -\mathbf{Q} + \mathbf{R}\mathbf{T}^{-1}\mathbf{R}' & -\mathbf{R}\mathbf{T}^{-1} \end{bmatrix}. \tag{15}$$

It has been proved [14] that if s is an eigenvalue of equation (14), so is $-s$. Therefore, we can assume that the first five eigenvalues have positive real parts (if the real part is zero, then we pick the eigenvalue with positive imaginary part) and the last five have opposite signs to the first five. We distinguish the corresponding 10 eigenvectors by attaching a subscript to $\mathbf{a}$ and $\mathbf{b}$. Then the general solution for the extended displacement and traction vectors (of the z-dependent, t-, x-, y-independent factor) are derived as

$$\begin{bmatrix} \mathbf{u} \\ \mathbf{t} \end{bmatrix} = \begin{bmatrix} \mathbf{A}_1 & \mathbf{A}_2 \\ \mathbf{B}_1 & \mathbf{B}_2 \end{bmatrix} \langle \mathrm{e}^{s^*z} \rangle \begin{bmatrix} \mathbf{K}_1 \\ \mathbf{K}_2 \end{bmatrix}, \tag{16}$$

where

$$\mathbf{A}_1 = [\mathbf{a}_1, \mathbf{a}_2, \mathbf{a}_3, \mathbf{a}_4, \mathbf{a}_5], \qquad \mathbf{A}_2 = [\mathbf{a}_6, \mathbf{a}_7, \mathbf{a}_8, \mathbf{a}_9, \mathbf{a}_{10}],$$

$$\mathbf{B}_1 = [\mathbf{b}_1, \mathbf{b}_2, \mathbf{b}_3, \mathbf{b}_4, \mathbf{b}_5], \qquad \mathbf{B}_2 = [\mathbf{b}_6, \mathbf{b}_7, \mathbf{b}_8, \mathbf{b}_9, \mathbf{b}_{10}],$$

$$\langle \mathrm{e}^{s^*z} \rangle = \mathrm{diag}\,[\mathrm{e}^{s_1z}, \mathrm{e}^{s_2z}, \mathrm{e}^{s_3z}, \mathrm{e}^{s_4z}, \mathrm{e}^{s_5z}, \mathrm{e}^{-s_1z}, \mathrm{e}^{-s_2z}, \mathrm{e}^{-s_3z}, \mathrm{e}^{-s_4z}, \mathrm{e}^{-s_5z}] \tag{17}$$

and $\mathbf{K}_1$ and $\mathbf{K}_2$ are 5×1 column matrices to be determined.

For a given frequency ω, equation (16) gives a general solution for the vibration of a homogeneous, magneto-electric-elastic, and simply supported plate. This solution contains previous piezoelectric and purely elastic solutions as its special cases. In spite of the complicated nature of the problem, the general solution is remarkably simple. For the special case of free vibration, the homogeneous boundary conditions at the top and bottom surfaces can be applied, from which the dispersion relation is obtained.

With equation (16) being served as a general solution for a homogeneous and magneto-electro-elastic plate, the solution for the corresponding layered plate can be derived using the continuity conditions along the interface and the homogeneous boundary conditions on the top and bottom surfaces of plate. In so doing, a system of linear equations for the unknowns can be formed and solved [3, 17]. For structures with relatively large numbers of layers (up to a hundred layers), however, the system of linear equations becomes very large, and the propagator matrix method developed exclusively for layered structures can be conveniently and efficiently applied (for a brief review, see reference [18]). We discuss this matter in the next section.

4. PROPAGATOR MATRIX AND SOLUTION FOR A LAYERED SYSTEM

Since the matrix $\mathbf{N}$, defined in equation (15), is not symmetric, the eigenvectors of equation (14) are actually the right ones. The left eigenvectors are found by solving the eigenvalue system

$$\mathbf{N}^{t}\boldsymbol{\eta} = \lambda\boldsymbol{\eta}. \tag{18}$$

It is a simple fact that if s and $[\mathbf{a}, \mathbf{b}]^{t}$ are the eigenvalue and eigenvector solutions of equation (14), then $\lambda = -s$ and $\boldsymbol{\eta} = [-\mathbf{b}, \mathbf{a}]^{t}$ are the corresponding solutions of equation (18). The orthogonality of the left and right eigenvectors yields the important relation

$$\begin{bmatrix} -\mathbf{B}_2^{t} & \mathbf{A}_2^{t} \\ \mathbf{B}_1^{t} & -\mathbf{A}_1^{t} \end{bmatrix} \begin{bmatrix} \mathbf{A}_1 & \mathbf{A}_2 \\ \mathbf{B}_1 & \mathbf{B}_2 \end{bmatrix} = \begin{bmatrix} \mathbf{I} & \mathbf{0} \\ \mathbf{0} & \mathbf{I} \end{bmatrix}, \tag{19}$$

where $\mathbf{I}$ is a 5×5 identity matrix, and the eigenvectors have been normalized according to

$$-\mathbf{B}_2^{t}\mathbf{A}_1 + \mathbf{A}_2^{t}\mathbf{B}_1 = \mathbf{I}. \tag{20}$$

Equation (19) resembles the orthogonal relation in the Stroh formalism [16] and provides us a simple way of inverting the eigenvector matrix, which is required in forming the propagator matrix.

Let us assume that equation (16) is a general solution in the homogeneous layer j, with the top and bottom boundaries being locally at $z = h$ and 0 respectively. Letting $z = 0$ in equation (16) and solving for the unknown column matrices, we find

$$\begin{bmatrix} \mathbf{K}_1 \\ \mathbf{K}_2 \end{bmatrix} = \begin{bmatrix} \mathbf{A}_1 & \mathbf{A}_2 \\ \mathbf{B}_1 & \mathbf{B}_2 \end{bmatrix}^{-1} \begin{bmatrix} \mathbf{u} \\ \mathbf{t} \end{bmatrix}_0 = \begin{bmatrix} -\mathbf{B}_2^{t} & \mathbf{A}_2^{t} \\ \mathbf{B}_1^{t} & -\mathbf{A}_1^{t} \end{bmatrix} \begin{bmatrix} \mathbf{u} \\ \mathbf{t} \end{bmatrix}_0. \tag{21}$$

The second equation follows from equation (19). Therefore, the solution in the homogeneous layer j at any z can be expressed by that at $z = 0$, i.e.,

$$\begin{bmatrix} \mathbf{u} \\ \mathbf{t} \end{bmatrix}_z = \mathbf{P}(z) \begin{bmatrix} \mathbf{u} \\ \mathbf{t} \end{bmatrix}_0, \tag{22}$$

where

$$\mathbf{P}(z) = \begin{bmatrix} \mathbf{A}_1 & \mathbf{A}_2 \\ \mathbf{B}_1 & \mathbf{B}_2 \end{bmatrix} \langle \mathrm{e}^{s^* z} \rangle \begin{bmatrix} -\mathbf{B}_2^{t} & \mathbf{A}_2^{t} \\ \mathbf{B}_1^{t} & -\mathbf{A}_1^{t} \end{bmatrix} \tag{23}$$

is called the propagator matrix [5, 18].

The propagating relation (23) can be used repeatedly so that we can propagate the physical quantities from the bottom surface $z = 0$ to the top surface $z = H$ of the layered plate. Consequently, we have

$$\begin{bmatrix} \mathbf{u} \\ \mathbf{t} \end{bmatrix}_H = \mathbf{P}_N(h_N)\mathbf{P}_{N-1}(h_{N-1}) \cdots \mathbf{P}_2(h_2)\mathbf{P}_1(h_1) \begin{bmatrix} \mathbf{u} \\ \mathbf{t} \end{bmatrix}_0, \tag{24}$$

where $h_j = z_{j+1} - z_j$ is the thickness of layer j and $\mathbf{P}_j$ the propagator matrix of layer j.

Equation (24) is a surprisingly simple relation and, for given homogeneous boundary conditions, can be reduced to the dispersion equation, from which the natural frequencies of the system can be solved. As an example, if we assume that the top and bottom surfaces are free boundaries (i.e., the elastic traction and the z-direction electric displacement and magnetic induction are zero), we then find

$$\begin{bmatrix} \mathbf{u}(H) \\ \mathbf{0} \end{bmatrix} = \begin{bmatrix} \mathbf{C}_1 & \mathbf{C}_2 \\ \mathbf{C}_3 & \mathbf{C}_4 \end{bmatrix} \begin{bmatrix} \mathbf{u}(0) \\ \mathbf{0} \end{bmatrix} \tag{25}$$

where the four submatrices $\mathbf{C}_j$ are obtained from the multiplication of the propagator matrices in equation (24). Therefore, the dispersion relation is simply the condition that the determinant of the submatrix $\mathbf{C}_3$ vanishes.

Similar dispersion relations can also be obtained for other combined free boundary conditions corresponding to the first-type and third-type (i.e., the mixed type) boundary value problems. Therefore, for the free vibration of an anisotropic, magneto-electro-elastic, simply supported, and multilayered rectangular plate, we have derived the analytical solution based on a new formalism similar to Stroh's [16] and the propagator matrix method.

5. NATURAL FREQUENCIES AND MODE SHAPES

Having derived the analytical solution, we now apply it to the study of natural frequencies and mode shapes in magneto-electro-elastic and multilayered plates.

First, a homogeneous, purely elastic, and orthotropic rectangular plate with its top and bottom surfaces being traction free is considered. This problem was analyzed by Srinivas and Rao [3] with the elastic constants C_{ij} being

$$[C] = \begin{bmatrix} 1 & 0{\cdot}23319 & 0{\cdot}010776 & 0 & 0 & 0 \\ & 0{\cdot}543103 & 0{\cdot}010776 & 0 & 0 & 0 \\ & & 0{\cdot}530172 & 0 & 0 & 0 \\ & & & 0{\cdot}26681 & 0 & 0 \\ & sym & & & 0{\cdot}159914 & 0 \\ & & & & & 0{\cdot}262931 \end{bmatrix}. \tag{26}$$

Listed in Table 1 are some of the symmetric and antisymmetric eigenvalues (or natural frequencies) for the given wavenumber (i.e., for given mH/L_x and nH/L_y) where the frequencies are normalized as $\Omega = \omega\sqrt{\rho H^2 C_{11}}$. It is clear that the present formulation predicts exactly the same natural frequencies as in Srinivas and Rao [3], even though a magneto-electro-elastic plate model has been used (with the coupling material coefficients e_{ik}, q_{ik}, and d_{ik} in equation (1) being set to zero).

TABLE 1

Normalized frequencies Ω in a purely elastic and orthotropic plate

		Srinivas and Rao [3]		Present	
mH/L_x	nH/L_y	*Anti*	*Sym*	*Anti*	*Sym*
0·1	0·1	0·04742	0·21697	0·04741896	0·21696691
0·1	0·2	0·10329	0·34501	0·10328951	0·34501431
0·1	0·3	0·18881	0·49530	0·18881038	0·49529880
0·2	0·1	0·11880	0·35150	0·11880052	0·35150232
0·2	0·2	0·16942	0·43382	0·16941500	0·43381816
0·2	0·3	0·24753	0·55201	0·24752548	0·55200611

TABLE 2

Piezoelectric material properties (E_i and G_{ii} are in GPa, e_{ij} in C/m^2, and $\varepsilon_0 = 8{\cdot}85 \times 10^{-12}/Fm$)

$E_1 = E_2$	E_3	v_{12}	$v_{13} = v_{23}$	$G_{44} = G_{55}$	G_{66}
81·3	64·5	0·329	0·432	25·6	30·6
$e_{24} = e_{15}$	$e_{31} = e_{32}$	e_{33}		$\varepsilon_{11}/\varepsilon_0 = \varepsilon_{22}/\varepsilon_0$	$\varepsilon_{33}/\varepsilon_0$
12·72	− 5·20	15·08		1475	1300

TABLE 3

Natural frequencies ω (in rad/(100 s)) in a homogeneous and piezoelectric plate

	Heyliger and Saravanos [19]		Present		
Mode	Case I	Case II	Case I	Case II	Elastic
1	713061	724602	713061·16	724602·30	616468·37
2	*777021*	*777021*	*777020·82*	*777020·82*	*777020·82*
3	889902	912912	889901·51	912911·99	839093·29
4	*925431*	*925431*	*925431·37*	*925431·37*	*925431·37*
5	1243819	*1270594*	1243819·29	*1270593·89*	1214012·58
6	*1270594*	1293504	*1270593·89*	1293503·71	*1270593·89*

Second, a homogeneous and piezoelectric plate is considered. The material properties are from Heyliger and Saravanos [19] and are given in Table 2. A unit density is assumed in this example. For $mH/L_x = nH/L_y = 1$ with $H = 0{\cdot}01$ m, the first six frequencies in rad/(100 s) are listed in Table 3 and compared to our previous results using a different analytical method. Boundary conditions on both the top and bottom surfaces are traction free and zero electric potential for case I, and traction free and zero electric displacement in the z-direction for case II. It is clear that the present method predicts exactly the same frequencies as those by Heyliger and Saravanos [19]. Furthermore, it is interesting to note that for both cases, three of the natural frequencies, two symmetric and one antisymmetric, are the same. Since these frequencies are actually the ones corresponding to the purely elastic plate as given in the last column of Table 2, we conclude that there are some vibration modes in the purely elastic media that are insensitive to the piezoelectric coupling.

This is actually true even for the case of piezoelectric/magnetostrictive sandwich plates to be studied next. Since these uncoupled elastic modes may be of particular interest to the analysis and design of smart structures, we first offer a brief physical explanation on these modes.

The differences in vibration mode between what one would compute with and without the coupling coefficients are a consequence of the stiffening effect that the piezoelectric and magnetostrictive terms generate when included in the physical problem. In general, these terms tend to increase the overall stiffness of the plate because of the internal forces generated by the induced electric and magnetic fields. There are certain vibration modes, however, for which the stain field is completely uncoupled from the piezoelectric and magnetostrictive coefficients. It is these modes that are, in fact, purely elastic and are independent of the coupling coefficients, and they arise because the elastic displacement field associated with these modes does not involve the integrated strain term that couples with electric and/or magnetic fields. These modes can be identified and isolated by simply analyzing the free vibration of the corresponding purely elastic plate, i.e., the magneto-electro-elastic plate with zero coupling coefficients (i.e., e_{ik}, q_{ik}, and d_{ik} are zero in equation (1)).

Having verified our formulation for the purely elastic and piezoelectric cases and discussed the purely elastic mode features, we now apply our solution to the sandwich plates made of the piezoelectric $BaTiO_3$ and the magnetostrictive $CoFe_2O_4$. The three layers are assumed to be of equal thickness of 0·1 m (with a total thickness $H = 0{\cdot}3$ m), and can be made of either $BaTiO_3$ or $CoFe_2O_4$. Material properties for the piezoelectric $BaTiO_3$ and magnetostrictive $CoFe_2O_4$ are listed, respectively, in Tables 4 and 5 [14, 20]. As can be seen,

TABLE 4

Material coefficients of the piezoelectric $BaTiO_3$ (C_{ij} in $10^9\,N/m^2$, e_{ij} in C/m^2, ε_{ij} in $10^{-9}\,C^2/N\,m^2$, and μ_{ij} in $10^{-6}\,N\,s^2/C^2$)

$C_{11} = C_{22}$	C_{12}	$C_{13} = C_{23}$	C_{33}	$C_{44} = C_{55}$	$C_{66} = 0{\cdot}5\,(C_{11}–C_{12})$
166	77	78	162	43	44·5
$e_{31} = e_{32}$	e_{33}	$e_{24} = e_{15}$			
− 4·4	18·6	11·6			
$\varepsilon_{11} = \varepsilon_{22}$	ε_{33}		$\mu_{11} = \mu_{22}$	μ_{33}	
11·2	12·6		5	10	

TABLE 5

Material coefficients of the magnetostrictive $CoFe_2O_4$ (C_{ij} in $10^9\,N/m^2$, q_{ij} in N/Am, ε_{ij} in $10^{-9}\,C^2/N\,m^2$, and μ_{ij} in $10^{-6}\,N\,s^2/C^2$)

$C_{11} = C_{22}$	C_{12}	$C_{13} = C_{23}$	C_{33}	$C_{44} = C_{55}$	$C_{66} = 0{\cdot}5\,(C_{11}–C_{12})$
286	173	170·5	269·5	45·3	56·5
$q_{31} = q_{32}$	q_{33}	$q_{24} = q_{15}$			
580·3	699·7	550			
$\varepsilon_{11} = \varepsilon_{22}$	ε_{33}		$\mu_{11} = \mu_{22}$	μ_{33}	
0·08	0·093		− 590	157	

TABLE 6

Normalized natural frequencies Ω in sandwich piezoelectric and magnetostrictive plate

Mode	B only	F only	B/F/B	F/B/F
1	2·3003336	1·9747225	1·8291326	1·9031079
2	4·0111017	3·3917316	3·1882709	3·2931003
3	5·8050002	4·6118448	4·4865902	4·5464350
4	7·2464901	5·4543731	5·3620531	5·6534567

both the piezoelectric $BaTiO_3$ and magnetostrictive $CoFe_2O_4$ are transversely isotropic with their symmetry axis being the z-axis. However, we remark that the magnetostrictive $CoFe_2O_4$ is dissipative in nature. That is, internal energy in such a system may not be always positive. The sandwich plates with stacking sequences $BaTiO_3/CoFe_2O_4/BaTiO_3$ (called B/F/B) and $CoFe_2O_4/BaTiO_3/CoFe_2O_4$ (called F/B/F) are investigated. For comparison, results for the homogeneous plate made of piezoelectric $BaTiO_3$ (i.e., with a B/B/B stacking and is called B only) and magnetostrictive $CoFe_2O_4$ (i.e., with an F/F/F stacking and is called F only) have been also studied. For simplicity, the densities for both $BaTiO_3$ and $CoFe_2O_4$ are assumed to be equal [21].

Listed in Table 6 are some of the lower eigenvalues (or natural frequencies) for these four cases. Boundary conditions on both the top and bottom surfaces are the extended traction free (i.e., the elastic traction, D_z, and B_z are zero). Also in Table 6, $mH/L_x = nH/L_y$ are fixed at 1·0, and the eigenvalues are normalized as $\Omega = \omega L_x/\sqrt{C_{max}/\rho_{max}}$ with C_{max} being the maximum of the C_{ij} in the whole sandwich plate and $\rho_{max} = 1$ being the maximum density in the system.

Comparing column 2 (B only) to column 3 (F only) of Table 6 for the same mode, we observed that the piezoelectric and magnetostrictive solids possess quite different natural frequencies. On the contrary, different stacking sequences of the truly sandwich plate have relatively close natural frequencies on the same mode, as can be seen by comparing column 4 (B/F/B) to column 5 (F/B/F).

Mode shapes corresponding to the frequencies given in Table 6 are plotted in Figures 1–4. In these figures, elastic displacements (u_x, u_y, u_z) are normalized by the maximum value in the whole thickness region for the three components, and the electric potential ϕ and magnetic potential ψ are normalized by their corresponding maximum value if they are different from zero.

Figure 1(a) and 1(b) are the symmetric mode shapes for the homogeneous and piezoelectric $BaTiO_3$ plate (B only) and for the sandwich $BaTiO_3/CoFe_2O_4/BaTiO_3$ (B/F/B), with frequency corresponding to mode 1 of Table 6. While the mode shapes for the homogeneous and magnetostrictive $CoFe_2O_4$ (F only) with frequency of mode 1 are exactly the same as the ones of B only, with the electric potential ϕ being replaced by the magnetic potential ψ, the mode shapes for the sandwich $CoFe_2O_4/BaTiO_3/CoFe_2O_4$ (F/B/F) with frequency of mode 1 have similar mode shapes as those for the B/F/B case (Figure 1(b)). For the sandwich F/B/F though, the horizontal elastic displacements u_x and u_y differ slightly from unit magnitude when reaching the top or bottom surface. Comparing the mode shapes for the four cases for the frequencies corresponding to mode 1, we conclude that mode 1 is a purely elastic mode, with its mode shapes being only slightly affected by the piezoelectric and magnetostrictive coupling.

Figure 2(a–d) show another set of symmetric mode shapes for the four cases corresponding to the frequencies of mode 2 of Table 6. It is clear that this mode is

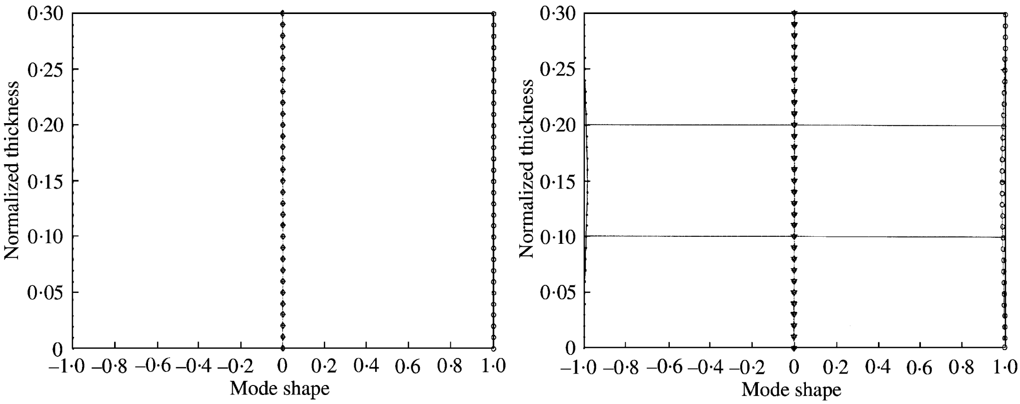

Figure 1. (a) Symmetric mode shapes for the homogeneous and piezoelectric $BaTiO_3$ plate (B only) with frequency corresponding to mode 1 of Table 6 ($\Omega = 2{\cdot}30$). Solid line with solid circle for u_x, dot line with open circle for u_y, dash dot line with open diamond for u_z, and dash line with a plus sign for ϕ; (b) Symmetric mode shapes for the sandwich $BaTiO_3/CoFe_2O_4/BaTiO_3$ (B/F/B) with frequency corresponding to mode 1 of Table 6 ($\Omega = 1{\cdot}83$). Solid line with solid circle for u_x, dot line with open circle for u_y, dash dot line with open diamond for u_z, dash line with a plus sign for ϕ, and dash line with open triangle for ψ.

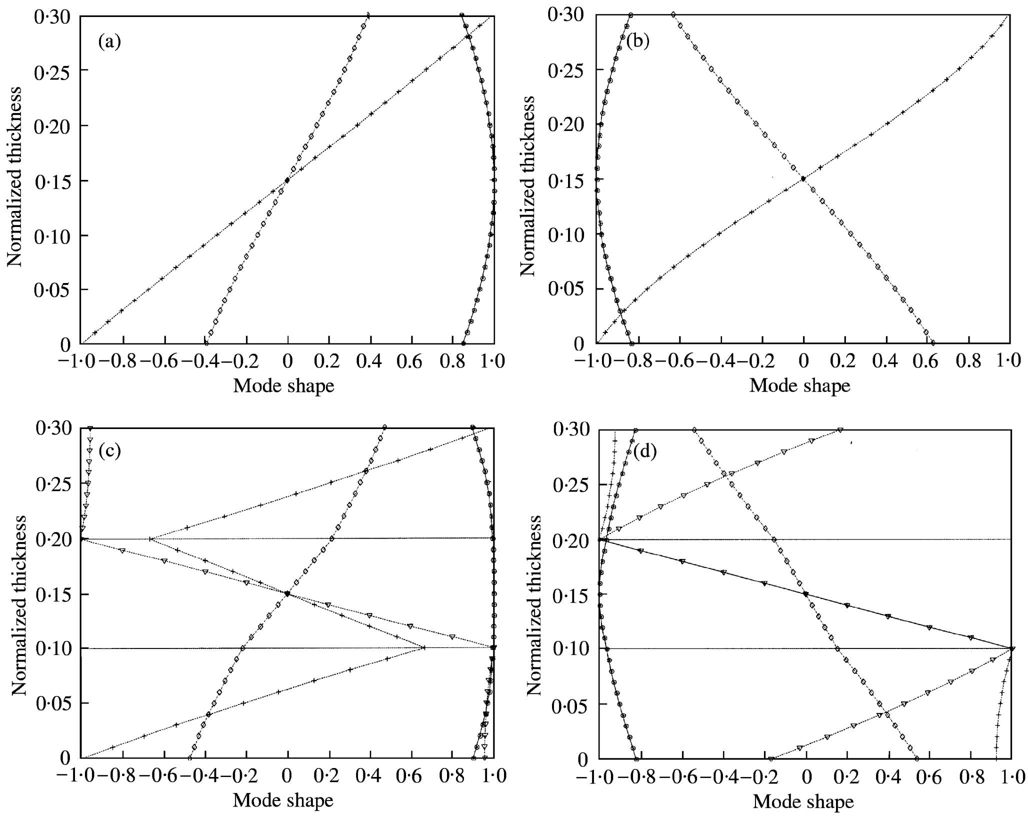

Figure 2. (a) Symmetric mode shapes for B only with frequency of mode 2 of Table 6 ($\Omega = 4{\cdot}01$). Solid line with solid circle for u_x, dot line with open circle for u_y, dash dot line with open diamond for u_z, and dash line with a plus sign for ϕ; (b) Symmetric mode shapes for F only with frequency of mode 2 of Table ($\Omega = 3{\cdot}39$). Solid line with solid circle for u_x, dot line with open circle for u_y, dash dot line with open diamond for u_z, dash line with a plus sign for ψ; (c) Symmetric mode shapes for B/F/B with frequency of mode 2 of Table 6 ($\Omega = 3{\cdot}19$). Solid line with solid circle for u_x, dot line with open circle for u_y, dash dot line with open diamond for u_z, dash line with a plus sign for ϕ, and dash line with open triangle for ψ; (d) Symmetric mode shapes for F/B/F with frequency of mode 2 of Table 6 ($\Omega = 3{\cdot}29$). Solid line with solid circle for u_x, dot line with open circle for u_y, dash dot line with open diamond for u_z, dash line with a plus sign for ϕ, and dash line with open triangle for ψ.

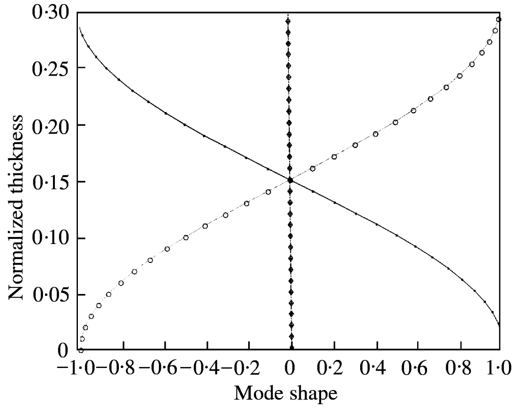

Figure 3. Antisymmetric mode shapes for B only with frequency of mode 3 of Table 6 ($\Omega = 5{\cdot}81$). Solid line with solid circle for u_x, dot line with open circle for u_y, dash dot line with open diamond for u_z, and dash line with a plus sign for ϕ.

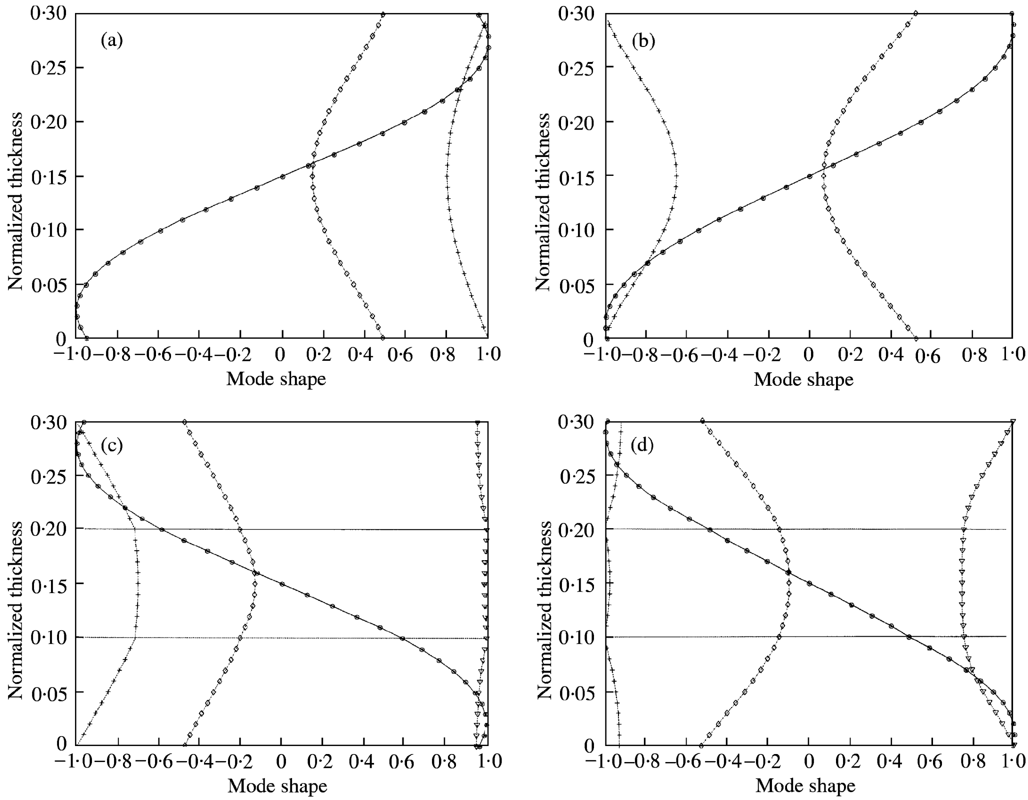

Figure 4. (a) Antisymmetric mode shapes for B only with frequency of mode 4 of Table 6 ($\Omega = 7{\cdot}25$). Solid line with solid circle for u_x, dot line with open circle for u_y, dash dot line with open diamond for u_z, and dash line with a plus sign for ϕ; (b) Antisymmetric mode shapes for F only with frequency of mode 4 of Table 6 ($\Omega = 5{\cdot}45$). Solid line with solid circle for u_x, dot line with open circle for u_y, dash dot line with open diamond for u_z, and dash line with a plus sign for ψ; (c) Antisymmetric mode shapes for B/F/B with frequency of mode 4 of Table 6 ($\Omega = 5{\cdot}36$). Solid line with solid circle for u_x, dot line with open circle for u_y, dash dot line with open diamond for u_z, dash line with a plus sign for ϕ, and dash line with open triangle for ψ; (d) Antisymmetric mode shapes for F/B/F with frequency of mode 4 of Table 6 ($\Omega = 5{\cdot}65$). Solid line with solid circle for u_x, dot line with open circle for u_y, dash dot line with open diamond for u_z, dash line with a plus sign for ϕ, and dash line with open triangle for ψ.

a piezoelectric/magnetostrictive mode, being very sensitive to either the material property or the stacking sequence. Especially, the electric and magnetic potentials are strongly influenced.

Shown in Figure 3 are the antisymmetric mode shapes for the B only case with the frequency corresponding to the mode 3 of Table 6. The mode shapes for the other three cases (i.e., F only, B/F/B, and F/B/F) are all nearly identical to those shown in Figure 3. Therefore, like mode 1, mode 3 is also a purely elastic mode.

Finally, Figure 4(a–d) show another set of antisymmetric mode shapes for the four cases corresponding to the frequencies of mode 4 of Table 6. Again, as for mode 2, this mode is very sensitive to either the material property or the stacking sequence.

6. CONCLUSIONS

In this paper, we have derived an analytical solution for the vibration of three-dimensional, anisotropic, magneto-electro-elastic, and multilayered rectangular plates with simply supported edges. This solution is a natural extension of the corresponding static solution developed recently by Pan [14]. On solving the vibration problem, the propagator matrix method and a simple formalism that resembles the Stroh formalism are proposed. The present solution includes all the previous solutions, such as the piezoelectric, piezomagnetic, purely elastic solutions as its special cases, and can provide benchmarks for various thick plate theories and numerical methods, such as the finite and boundary element methods.

Typical numerical examples are presented for the purely elastic, piezoelectric and magnetostrictive rectangular plates. For the free vibration of a homogeneous and purely elastic plate, we found that the natural frequencies obtained by the present solution are in exact agreement with the previous ones, even though a homogeneous and piezoelectric/magnetostrictive plate (with uncoupled material coefficients) was used in the present formulation. For a homogeneous and piezoelectric plate, the natural frequencies (under different electric boundary conditions on the top and bottom surfaces) obtained by the present solution are again in exact agreement with our previous results based on a different analytical method. Furthermore, we have observed that half of the piezoelectric frequencies have exactly the same values as their purely elastic counterpart. In other words, piezoelectric coupling has effect on only half of the purely elastic modes, a complicated stiffening effect discussed in the previous section.

For the four cases of the sandwich piezoelectric/magnetostrictive plate (B only, F only B/F/B, and F/B/F), we observed the following features:

(1) On the same mode, the natural frequencies for the four cases are quite different, especially, for the B only and F only cases.
(2) Some of the modes are purely elastic. That is, piezoelectric/magnetostrictive coupling does not produce electric and magnetic potentials, and the elastic displacements are nearly identical in both the purely elastic and piezoelectric/magnetostrictive cases. Again, that is the stiffening effect generated by the piezoelectric and magnetostrictive terms.
(3) For the piezoelectric/magnetostrictive coupling mode, all the mode shapes, especially the elastic displacement component in the z-direction and electric and magnetic potentials depend strongly upon the material properties and stacking sequences.

These significant and interesting features will be particularly useful in the analysis and design of magneto-electro-elastic composite laminates, and for a given stacking sequence of the composite laminate, the present analytical solution offers a simple and accurate tool for the prediction, identification, and study of these features.

ACKNOWLEDGMENTS

The authors would like to thank Professor Joseph Dougherty of PenState for kindly providing information on the material densities for the piezoelectric $BaTiO_3$ and magnetostrictive $CoFe_2O_4$.

REFERENCES

1. O. O. OCHOA and J. N. REDDY 1992 *Finite Element Analysis of Composite Laminates*. Boston, MA: Kluwer Academic Publishers.
2. S. SRINIVAS, C. V. J. RAO and A. K. RAO 1970 *Journal of Sound and Vibration* **12**, 187–199. An exact analysis for vibration of simply-supported homogeneous and laminated thick rectangular plates.
3. S. SRINIVAS and A. K. RAO 1970 *International Journal of Solids and Structures* **6**, 1463–1481. Bending, vibration and buckling of simply supported thick orthotropic rectangular plates and laminates.
4. E. PAN 1992 *Journal of Elasticity* **27**, 167–181. Vibration of a transversely isotropic, simply supported and layered rectangular plates.
5. F. GILBERT and G. BACKUS 1966 *Geophysics* **31**, 326–332. Propagator matrices in elastic wave and vibration problems.
6. A. K. NOOR and W. S. BURTON 1990 *Journal of Applied Mechanics* **57**, 182–188. Three-dimensional solutions for antisymmetrically laminated anisotropic plates.
7. M. C. RAY, K. M. RAO and B. SAMANTA 1992 *Computers and Structures* **45**, 667–677. Exact analysis of coupled electroelastic behavior of a piezoelectric plate under cylindrical bending.
8. M. C. RAY, R. BHATTACHARYA and B. SAMANTA 1993 *American Institute of Aeronautics and Astronautics Journal* **31**, 1684–1691. Exact solutions for static analysis of intelligent structures.
9. P. R. HEYLIGER and S. P. BROOKS 1995 *International Journal of Solids and Structures* **32**, 2945–2959. Free vibration of piezoelectric laminates in cylindrical bending.
10. W. SMITTAKORN and P. R. HEYLIGER 2000 *Mechanics of Composite Materials and Structures* **7,** 79–104. A discrete-layer model of laminated hygrothermopiezoelectric plates.
11. G. HARSHE, J. P. DOUGHERTY and R. E. NEWNHAM 1993 *International Journal of Applied Electromagnetic Materials* **4**, 145–159. Theoretical modeling of multiplayer magnetoelectric composites.
12. C. W. NAN 1994 *Physical Review B* **50**, 6082–6088. Magnetoelectric effect in composites of piezoelectric and piezomagnetic phases.
13. Y. BENVENISTE 1995 *Physical Review B* **51**, 16 424–16 427. Magnetoelectric effect in fibrous composites with piezoelectric and piezomagnetic phases.
14. E. PAN 2001 *Journal of Applied Mechanics* **68**, 608–618. Exact solution for simply supported and multilayered magneto-electro-elastic plates.
15. A. N. STROH 1958 *Philosophical Magazine* **3**, 625–646. Dislocations and cracks in anisotropic elasticity.
16. T. C. T. TING 1996 *Anisotropic Elasticity*. Oxford: Oxford University Press.
17. A. T. JONES 1971 *Journal of Composite Materials* **5**, 504–520. Exact natural frequencies and modal functions for a thick off-axis lamina.
18. E. PAN 1997 *Applied Mathematical Modelling* **21**, 509–521. Static Green's functions in multilayered half spaces.
19. P. R. HEYLIGER and D. A. SARAVANOS 1995 *Journal of Acoustic Society of America* **98**, 1547–1557. Exact free vibration analysis of laminated plates with embedded piezoelectric layers.
20. J. H. HUANG and W. S. KUO 1997 *Journal of Applied Physics* **81**, 1378–1386. The analysis of piezoelectric/piezomagnetic composite materials containing ellipsoidal inclusions.
21. D. A. BERLINGCOURT, D. R. CURRAN and H. JAFFE 1964 *Physical Acoustics* **1**, 169–270. Piezoelectric and piezomagnetic materials and their function in transducers.